

Controlled Formation of Carbon Nanotube Junctions via Linker-Induced Assembly in Aqueous Solution

Matteo Palma,^{*,†} Wei Wang,[‡] Erika Penzo,[†] Julian Brathwaite,[§] Ming Zheng,^{||} James Hone,[§] Colin Nuckolls,[‡] and Shalom J. Wind^{*,†}

Departments of [†]Applied Physics and Applied Mathematics, [‡]Chemistry, and [§]Mechanical Engineering, Columbia University, New York, New York 10027, United States

^{||}Polymers Division, National Institute of Standards and Technology, 100 Bureau Drive, Gaithersburg, Maryland 20899-8542, United States

S Supporting Information

ABSTRACT: Here we present a simple approach for the controlled formation of one-dimensional and multi-terminal nanotube junctions. We describe a facile bottom-up strategy for joining the ends of single-walled carbon nanotubes. The geometry of the junctions can be varied and controlled by linker-induced assembly of DNA-wrapped nanotubes.

Here we present a simple bottom-up approach for the controlled formation of end-to-end single-walled carbon nanotube (SWCNT) junctions via directed chemical reactions. CNT-based nanoscale devices require junctions among different nanotubes as well as between CNTs and functional molecules/moieties.^{1–8} In particular, junctions obtained from SWCNTs are of interest for nanoscale electronic devices because of the nanoscale diameter of the tubes and their room-temperature transport properties. SWCNT/SWCNT junctions have been observed in samples produced with different techniques, such as chemical vapor deposition (CVD),^{9–11} laser ablation,⁴ and electrical welding.¹² Additionally, multi-terminal SWCNT junctions have been irregularly produced by arc discharge,¹³ laser ablation,¹⁴ CVD,¹⁵ and electron-beam welding.¹⁶ Ringlike CNTs have also been synthesized by several methods, such as covalent ring-closure reactions,¹⁷ non-covalent interactions,^{18–20} the floating CVD method,²¹ and electron-beam irradiation.^{22,23}

CNTs have been further interconnected via chemical functionalization in solution,^{17–19,24–28} but this has been done without effective control over the junction formation (end-to-end and/or end-to-side). Recent studies by Swager and co-workers produced SWCNTs terminally linked by oligonucleotides into a nanowire motif, employing a side-wall protection step to overcome regiospecific SWCNT covalent attachment.²⁹

In the study presented here, we directed chemical reactions to occur at the ends of well-defined segments of SWCNTs to form junctions of end-to-end-linked tubes. We further found that linkers with different shapes yield SWCNTs with higher-order structures that go beyond simple linear arrays to ones that are multiterminal and circular. These unusual structures were formed from a self-assembly process in aqueous solution

that is controlled by the geometry and the chemical nature of the linker.

The SWCNTs used in this study were sonicated and dispersed in water via side-wall interactions with single-stranded DNA [see the Supporting Information (SI)].³⁰ DNA-assisted dispersion of SWCNTs enables nanotube separation by chirality and electronic structure (i.e., metallic vs semiconducting).³¹ The helical wrapping of the SWCNTs with DNA further allows the separation of nanotubes by length via size-exclusion chromatography.³² Moreover, this method leaves only the terminal ends of the SWCNTs available for direct functionalization.

SWCNTs sonicated in water exhibit functional groups as a result of the use of ultrasound when preparing the suspension.³³ •H atoms and •OH radicals are in fact generated upon sonication in aqueous solutions and can then either combine to form H₂, H₂O₂, and water or attack solute molecules, which can therefore be oxidized.³⁴ The presence of carboxylic acid groups on the terminal ends of our nanotubes was further supported by the observed immobilization of activated nanotubes on amine-functionalized (nano)patterns (see the SI and Figure SI-1). We exploited this selectivity to link SWCNTs in amidation reactions with amino-functionalized molecular linkers to form *only* end-to-end junctions.

Figure 1 depicts the three different molecular linkers used for this purpose (labeled A, B, and C). Varying the type of linker allowed us to create either linear (A) or multiterminal (B, C) SWCNT junctions, where the geometry of the junction was dictated by the chemical and geometrical nature of the linker. The SWCNT carboxylic acid end groups were activated in buffer solutions containing standard amide coupling and activating agents (Sulfo-NHS and EDCI, respectively;³⁵ see the SI for experimental details). This chemistry covalently connects the amine-functionalized molecules to the end of the nanotubes via an amidation reaction. Employing diamine molecular bridges, we were able to link different SWCNT segments via a simple reaction strategy in environmentally friendly aqueous solutions. The molecular linkers employed presented multiple amine functionalities for bridging of two or more SWCNTs.

Received: February 19, 2013

Published: May 8, 2013

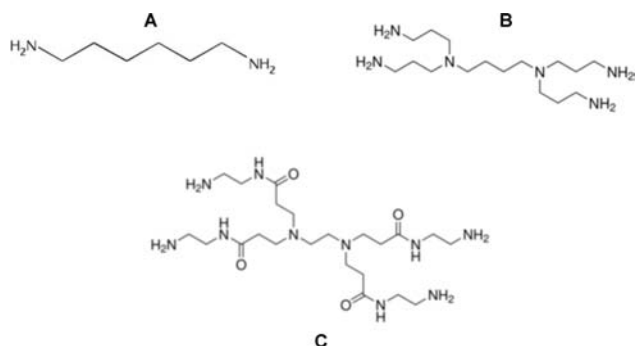


Figure 1. The three different molecular linkers employed: (A) hexamethylenediamine; (B) polypropylenimine tetramine dendrimer; (C) poly(amidoamine) (PAMAM) dendrimer with an ethylenediamine core.

To determine the degree of coupling and to monitor the self-assembly, we cast low-coverage films on silicon wafer substrates and imaged them with atomic force microscopy (AFM) and transmission electron microscopy (TEM). The starting SWCNTs before reaction had an average length of 147.7 ± 92.8 nm (Figure 2).

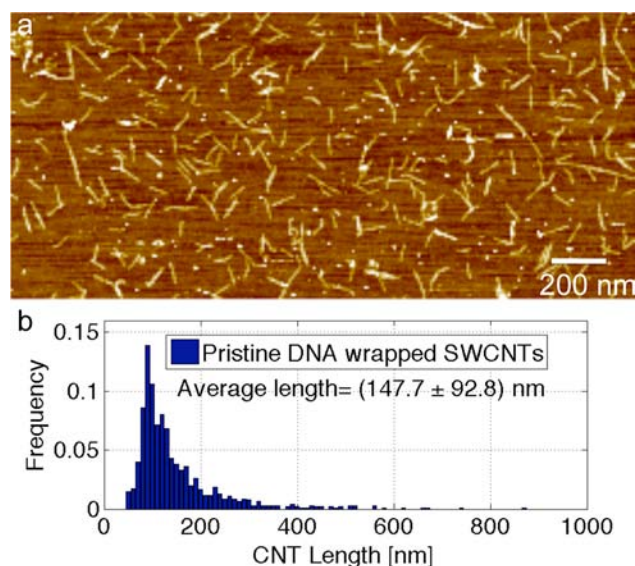


Figure 2. (a) AFM topographical image of pristine DNA-wrapped SWCNTs. (b) Normalized histogram showing the length distribution of the pristine DNA-wrapped SWCNTs. The average length of 147.7 ± 92.8 nm was determined from ca. 900 SWCNTs.

Figure 3a,b shows AFM and TEM images of linear SWCNT junctions typically obtained employing molecule A as the linker. The average length of the SWCNTs segments was found to increase from 147.7 ± 92.8 nm for the pristine DNA-wrapped SWCNTs (starting material; see the histogram in Figure 2b) to 418.2 ± 370.1 nm when linear molecule A was allowed to react with (i.e., bridge) SWCNTs in solution (Figure 3c). This significant increase in the average length of the SWCNTs visualized on the substrate surface indicates the formation of linear SWCNT junctions (also see Figures SI-2 and SI-3).^{36,37}

To create multiterminal SWCNT junctions, we employed branched molecular bridges to interconnect pristine SWCNTs via the above-described functionalization strategy (i.e.,

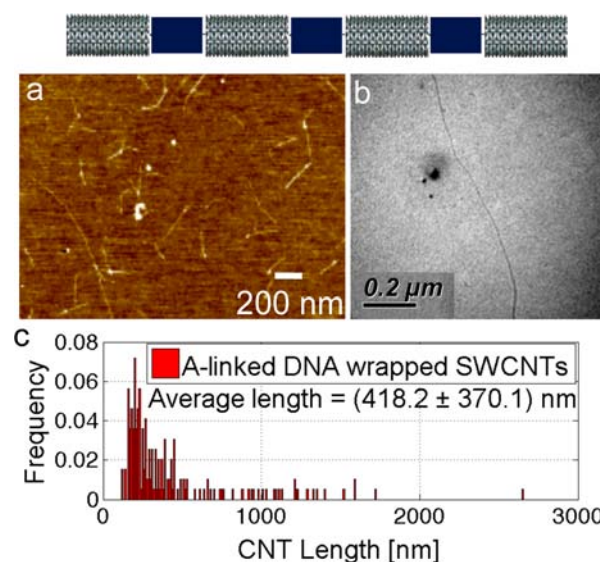


Figure 3. (top) Schematic of linear end-to-end SWCNT junctions. (a) AFM topographical image and (b) TEM image of linear end-to-end SWCNT junctions formed using molecular linker A. (c) Normalized histogram showing the length distribution of the observed linear junctions. The average length of 418.2 ± 370.1 nm was determined from ca. 200 nanotube junctions.

amidation). Figure 4a,b shows various multiterminal SWCNT junctions formed using linker B (also see Figure SI-4). These Y-shaped junctions predominantly exhibit the same height of the pristine SWCNTs (ca. 1.2 nm) and thus are the result of nanotube interconnections. The tubes in these junctions exhibited an average length of 522.5 ± 351.4 nm (see the

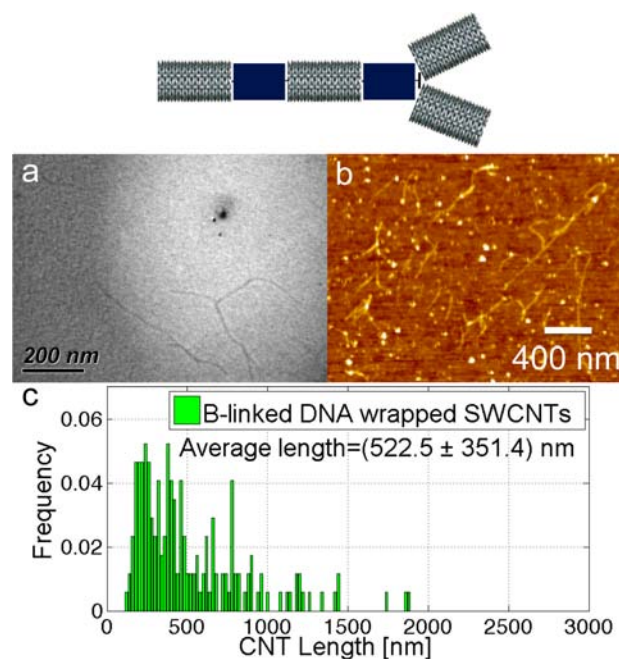


Figure 4. (top) Schematic of a Y-shaped end-to-end SWCNT junction. (a) TEM image and (b) AFM topographical image of multiterminal end-to-end SWCNT junctions formed using molecular linker B. (c) Normalized histogram showing the length distribution of the observed B-linked SWCNTs. The average length of 522.5 ± 351.4 nm was determined from ca. 200 nanotube junctions.

histogram in Figure 4c). Notably, junctions such as these are of interest for the creation of three-terminal nanotransistors.²⁵

We further employed linker C as a molecular bridge in SWCNT junction formation. The longer branched chains minimize steric hindrance effects upon amidation of two or more SWCNTs; furthermore the amide functional groups can induce hydrogen-bond formation among different molecules/linkers and therefore add an extra non-covalent stabilizing effect. Figure 5a shows a TEM image of typical multiterminal

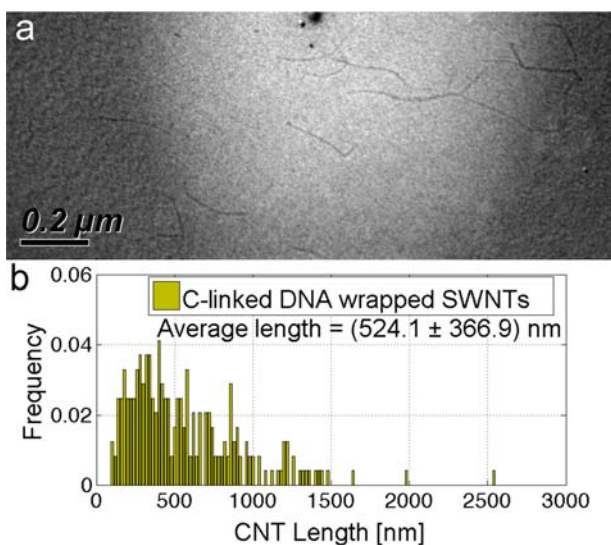


Figure 5. Schematic of a Y-shaped end-to-end SWCNT junction. (a) TEM image of multibranch end-to-end SWCNT junctions formed using molecular linker C. (b) Normalized histogram showing the length distribution for the observed C-linked SWCNTs. The average length of 524.1 ± 366.9 nm was determined from ca. 200 nanotube junctions.

junctions observed when linker C was employed (also see Figure SI-5). The average length of such junctions was determined to be 524.1 ± 366.9 nm, as shown in the histogram in Figure 5b.

When molecular bridge C was employed, we found evidence of side-to-side interactions among multiple SWCNTs (Figure 6a). We also observed ringlike assemblies from the same solutions; Figure 6b depicts such case (also see Figure SI-6). Parallel nanotube arrays can be useful for high-performance electronics applications, and there is indeed an interest in inducing such assemblies.³⁸ Moreover, ringlike structures can be potentially valuable as quantum interferometers for the production of tunable nanoscale electronic switching devices.^{22,39} The SWCNT assemblies we observed using molecular bridge C (see Figure 6) are likely to be stabilized by an interplay between van der Waals interactions and hydrogen-bond formation among linkers bridging the nanotubes.⁴⁰ It is noteworthy that when trifluoroacetic acid was added to the SWCNT solution to disrupt the hydrogen-bond formation among molecular linkers C belonging to different SWCNT junctions, no linear nor circular side-to-side assemblies were observed.

In summary, we have presented a facile and green strategy for fabricating linear and multiterminal carbon nanotube junctions using end-to-end linking of SWCNTs and subsequent linker-induced assembly. Furthermore, non-covalent interactions between molecular bridges have been shown to allow for the

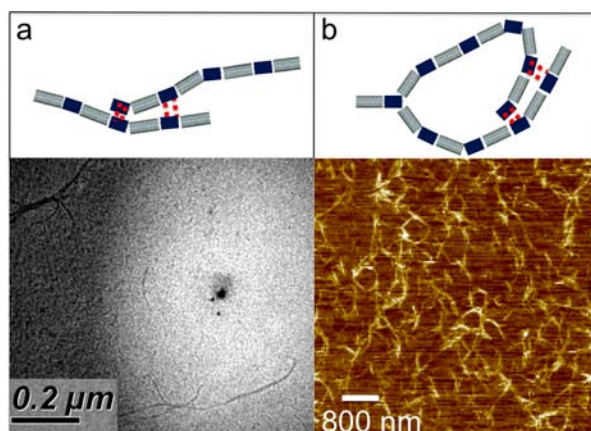


Figure 6. SWCNT assemblies employing molecule C as the linker. (a) Schematic and TEM image of parallel SWCNT architectures and (shown as red dashes) the possible van der Waals and hydrogen-bond interactions among C linkers involved in their formation. (b) Schematic and AFM topographical image of circular SWCNT assemblies. The average diameter of the observed ringlike architectures was found to be 408.1 ± 100.2 nm.

formation of parallel and ringlike SWCNT assemblies. The approach presented is of general applicability for the sustainable fabrication of solution-processable CNT-based nanoscale devices. Three-terminal connections to molecules can be used, for example, for the development of individually gated molecular logic devices. Moreover, the strategy presented here can be utilized to selectively dope (and therefore increase the conductivity) of semiconductor SWCNT networks by employing functional groups that can act as electron donors/acceptors.

■ ASSOCIATED CONTENT

📄 Supporting Information

Experimental procedures, AFM and TEM images, and data analysis. This material is available free of charge via the Internet at <http://pubs.acs.org>.

■ AUTHOR INFORMATION

✉ Corresponding Author

mp2766@columbia.edu; sw2128@columbia.edu

Notes

The authors declare no competing financial interest.

■ ACKNOWLEDGMENTS

We gratefully acknowledge financial support from the Office of Naval Research (N00014-09-1-1117). Additional support from the Nanoscale Science and Engineering Initiative of the National Science Foundation (CHE-0641523) and from the New York State Office of Science, Technology, and Academic Research (NYSTAR) is also gratefully acknowledged.

■ REFERENCES

- (1) Saito, S. *Science* **1997**, *278*, 77.
- (2) Yao, Z.; Postma, H. W. C.; Balents, L.; Dekker, C. *Nature* **1999**, *402*, 273.
- (3) Fuhrer, M. S.; Nygard, J.; Shih, L.; Forero, M.; Yoon, Y. G.; Mazzone, M. S. C.; Choi, H. J.; Ihm, J.; Louie, S. G.; Zettl, A.; McEuen, P. L. *Science* **2000**, *288*, 494.
- (4) Ouyang, M.; Huang, J. L.; Cheung, C. L.; Lieber, C. M. *Science* **2001**, *291*, 97.

(5) Bandaru, P. R.; Daraio, C.; Jin, S.; Rao, A. M. *Nat. Mater.* **2005**, *4*, 663.

(6) Yao, Y. G.; Li, Q. W.; Zhang, J.; Liu, R.; Jiao, L. Y.; Zhu, Y. T.; Liu, Z. F. *Nat. Mater.* **2007**, *6*, 283.

(7) Wei, D. C.; Liu, Y. Q. *Adv. Mater.* **2008**, *20*, 2815.

(8) Peng, X. H.; Misewich, J. A.; Wong, S. S.; Sfeir, M. Y. *Nano Lett.* **2011**, *11*, 4562.

(9) Doorn, S. K.; O'Connell, M. J.; Zheng, L. X.; Zhu, Y. T.; Huang, S. M.; Liu, J. *Phys. Rev. Lett.* **2005**, *94*, No. 016802.

(10) Han, J.; Anantram, M. P.; Jaffe, R. L.; Kong, J.; Dai, H. *Phys. Rev. B* **1998**, *57*, 14983.

(11) Ruppalt, L. B.; Lyding, J. W. *Small* **2007**, *3*, 280.

(12) Jin, C. H.; Suenaga, K.; Iijima, S. *Nat. Nanotechnol.* **2008**, *3*, 17.

(13) Osvath, Z.; Koos, A. A.; Horvath, Z. E.; Gyulai, J.; Benito, A. M.; Martinez, M. T.; Maser, W. K.; Biro, L. P. *Chem. Phys. Lett.* **2002**, *365*, 338.

(14) Chiu, P. W.; Roth, S. *Appl. Phys. Lett.* **2007**, *91*, No. 102109.

(15) Liu, L. W.; Fang, J. H.; Lu, L.; Zhou, F.; Yang, H. F.; Jin, A. Z.; Gu, C. Z. *Phys. Rev. B* **2005**, *71*, 155.

(16) Terrones, M.; Banhart, F.; Grobert, N.; Charlier, J. C.; Terrones, H.; Ajayan, P. M. *Phys. Rev. Lett.* **2002**, *89*, No. 075505.

(17) Sano, M.; Kamino, A.; Okamura, J.; Shinkai, S. *Science* **2001**, *293*, 1299.

(18) Martel, R.; Shea, H. R.; Avouris, P. *Nature* **1999**, *398*, 299.

(19) Geng, J. X.; Ko, Y. K.; Youn, S. C.; Kim, Y. H.; Kim, S. A.; Jung, D. H.; Jung, H. T. *J. Phys. Chem. C* **2008**, *112*, 12264.

(20) Singh, P.; Toma, F. M.; Kumar, J.; Venkatesh, V.; Raya, J.; Prato, M.; Verma, S.; Bianco, A. *Chem.—Eur. J.* **2011**, *17*, 6772.

(21) Song, L.; Ci, L. J.; Sun, L. F.; Jin, C. H.; Liu, L. F.; Ma, W. J.; Liu, D. F.; Zhao, X. W.; Luo, S. D.; Zhang, Z. X.; Xiang, Y. J.; Zhou, J. J.; Zhou, W. Y.; Ding, Y.; Wang, Z. L.; Xie, S. S. *Adv. Mater.* **2006**, *18*, 1817.

(22) Grimm, D.; Venezuela, P.; Banhart, F.; Grobert, N.; Terrones, H.; Ajayan, P. M.; Terrones, M.; Latge, A. *Small* **2007**, *3*, 1900.

(23) Terrones, M.; Terrones, H.; Banhart, F.; Charlier, J. C.; Ajayan, P. M. *Science* **2000**, *288*, 1226.

(24) Chiu, P.-W.; Duesberg, G. S.; Dettlaff-Weglikowska, U.; Roth, S. *Appl. Phys. Lett.* **2002**, *80*, 3811.

(25) Chiu, P.-W.; Kaempgen, M.; Roth, S. *Phys. Rev. Lett.* **2004**, *92*, No. 246802.

(26) Cao, L.; Yang, W.; Yang, J. W.; Wang, C. C.; Fu, S. K. *Chem. Lett.* **2004**, *33*, 490.

(27) Frehill, F.; Vos, J. G.; Benrezzak, S.; Koos, A. A.; Konya, Z.; Ruther, M. G.; Blau, W. J.; Fonseca, A.; Nagy, J. B.; Biro, L. P.; Minett, A. I.; Panhuis, M. I. H. *J. Am. Chem. Soc.* **2002**, *124*, 13694.

(28) Lyonnais, S.; Chung, C. L.; Goux-Capes, L.; Escude, C.; Pietrement, O.; Baconnais, S.; Le Cam, E.; Bourgoin, J. P.; Filoramo, A. *Chem. Commun.* **2009**, 683.

(29) Weizmann, Y.; Chenoweth, D. M.; Swager, T. M. *J. Am. Chem. Soc.* **2010**, *132*, 14009.

(30) Zheng, M.; Jagota, A.; Semke, E. D.; Diner, B. A.; Mclean, R. S.; Lustig, S. R.; Richardson, R. E.; Tassi, N. G. *Nat. Mater.* **2003**, *2*, 338.

(31) Tu, X. M.; Manohar, S.; Jagota, A.; Zheng, M. *Nature* **2009**, *460*, 250.

(32) Huang, X. Y.; McLean, R. S.; Zheng, M. *Anal. Chem.* **2005**, *77*, 6225.

(33) Kaempgen, M.; Lebert, M.; Haluska, M.; Nicoloso, N.; Roth, S. *Adv. Mater.* **2008**, *20*, 616.

(34) Riesz, P.; Kondo, T. *Free Radical Biol. Med.* **1992**, *13*, 247.

(35) Guo, X. F.; Gorodetsky, A. A.; Hone, J.; Barton, J. K.; Nuckolls, C. *Nat. Nanotechnol.* **2008**, *3*, 163.

(36) To verify that an amidation reaction and not a supramolecular interaction is actually responsible for the formation of SWCNT junctions, we measured the length of the SWCNTs after addition of the diamine molecular linker/s without the amide coupling and activating agents (Sulfo-NHS and EDCI). The average nanotube length in this case was comparable to that of the pristine SWCNTs, thus indicating that the amidation reaction is the main driving force for

the formation of SWCNT junctions (see the SI and Figure SI-3 for a more detailed discussion).

(37) The presence of unreacted species cannot be excluded. Even after the reaction, we observed nanotubes with lengths comparable to those of single pristine tubes, as evidenced by the nanotubes length distribution in Figure 3c.

(38) Han, S.-p.; Maune, H. T.; Barish, R. D.; Bockrath, M.; Goddard, W. A., III. *Nano Lett.* **2012**, *12*, 1129.

(39) Grimm, D.; Muniz, R. B.; Latge, A. *Phys. Rev. B* **2003**, *68*, No. 193407.

(40) Bubble formation might also be involved in inducing the assembly of SWCNTs into circular architectures and cannot be excluded a priori (see ref 18).